XXXth IAU General Assembly, August 2018
Chanda Jog & Danail Obreschkow, ed.
DOI: 10.5281/zenodo.1481579

Connecting Angular Momentum, Mass, and Morphology: Insights from the Magneticum Simulations

Rhea-Silvia Remus[1], Adelheid F. Teklu[1,2], Felix Schulze[1,3], and Klaus Dolag[1,4]

[1]Universitäts-Sternwarte München, Scheinerstr. 1, D-81679 München, Germany
[2]Excellence Cluster Universe, Boltzmannstr. 2, D-85748 Garching, Germany
[3]MPI for Extraterrestrial Physics, P.O. Box 1312, D-85748 Garching, Germany
[4]MPI for Astrophysics, Karl-Schwarzschild Strasse 1, D-85748 Garching, Germany
email: rhea@usm.lmu.de

Abstract. Understanding the connection between the angular momentum properties of a galaxy and its formation history and thus its morphological properties is one of the most intriguing quests in extragalactic astrophysics. State-of-the-art hydrodynamical cosmological simulations of large volumes with sufficient resolution to trace the properties of an entire population of galaxies with a large range of masses are essential to disentangle the different processes in galaxy formation that lead to the huge variety in morphological and kinematical properties observed in present-day galaxies, but such simulations only recently became available. One such set of simulations is Magneticum Pathfinder. We present insights obtained from these simulations with regard to the close connection between the angular momentum, the stellar mass, and the morphology of galaxies. Here, we demonstrate that the position of a galaxy in the M_*–j_* plane, described by the so-called b-value (see Teklu et al. 2015), is an excellent tracer for the morphology of a galaxy, visible also in the mass–size relation, the λ_R–ϵ plane, and other galaxy properties. This clearly highlights the importance of observational measurements of the angular momentum of galaxies, even though they are difficult to obtain. We conclude that using the b-value to classify galaxies is an extremely powerful tool for both simulations and observations.

Keywords. galaxies: kinematics and dynamics – galaxies: elliptical – galaxies: spiral – methods: numerical

1. The Magneticum Pathfinder Simulations

The *Mageticum Pathfinder* simulation suite (**www.magneticum.org**, Dolag et al., in prep., see also Hirschmann et al. 2014; Steinborn et al. 2015 for more details) consists of several hydrodynamical cosmological boxes with volumes ranging from $(2688\ h^{-1}\mathrm{Mpc})^3$ to $(18\ h^{-1}\mathrm{Mpc})^3$ with different resolutions. They were performed with a modified version of GADGET (Springel 2005), including radiative cooling, star formation, and kinetic winds (Springel & Hernquist 2003), stellar evolution and metal enrichment (Tornatore et al. 2007), and black hole feedback (Springel et al. 2005; Hirschmann et al. 2014). Furthermore, special treatment of artificial viscosity to resolve turbulent motion (Dolag et al. 2005) and thermal conduction (Dolag et al. 2004) are included. For all simulations, a WMAP7 (Komatsu et al. 2011) ΛCDM cosmology with $h = 0.704$, $\Omega_m = 0.272$, and $\Lambda = 0.728$ was adopted. Galaxies within the simulations are identified with the baryonic SUBFIND version (Springel et al. 2001; Dolag et al. 2009).

To study galaxies in detail, we use a medium-sized box (Box4, $(48\ h^{-1}\mathrm{Mpc})^3$) with a resolution of $M_{\mathrm{DM}} = 3.6 \times 10^7\, h^{-1} M_\odot$ and $M_{\mathrm{Gas}} = 7.3 \times 10^6\, h^{-1} M_\odot$. Each gas particle spawns up to four star particles, and the softening for the stars is $\epsilon_* = 0.7\, h^{-1}\mathrm{kpc}$. The

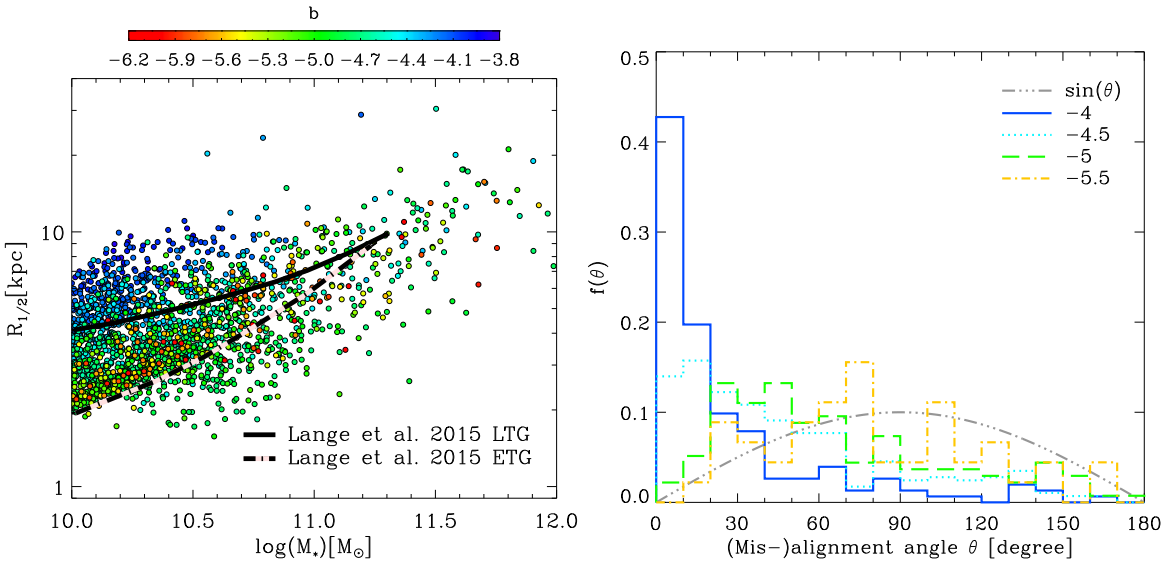

Figure 1. *Left panel:* The mass–size relation for all galaxies from Magneticum Box4, colored according to their b-value calculated as in Eq. 2.1, at $z = 0$. Black lines show the observed relations for late- (solid line) and early-type (dashed line) galaxies derived by Lange et al. (2015) from the GAMA survey. *Right panel:* Histograms of the angle between the angular momentum axes of the stellar and cold gas components of the galaxies from Magneticum Box4, for different b-value bins. The blue solid line shows the histogram for galaxies classified as disks according to their b-value, and the orange dash-dotted line shows the histogram for galaxies classified as spheroidals. The gray dash-dot-dot-dotted line marks a random distribution of the angles.

properties of the galaxies from this box have been shown to excellently reproduce the observed galaxy properties of both disk and spheroidal galaxies (e.g., Teklu et al. 2015; Remus et al. 2015; Teklu et al. 2016, 2017; Remus et al. 2017; Schulze et al. 2018).

2. Morphological Classification with the M_*–j_* Plane

As demonstrated by Teklu et al. (2015), the Magneticum galaxies successfully reproduce the observed distribution of galaxies in the M_*–j_* plane (Fall & Romanowsky 2013). The position of a galaxy in this plane can be described by the b-value:

$$b = \log_{10}\left(\frac{j_*}{\text{kpc km s}^{-1}}\right) - \frac{2}{3}\log_{10}\left(\frac{M_*}{M_\odot}\right), \tag{2.1}$$

the y-intercept of a linear function with slope 2/3 in the $\log_{10}(M_*)$–$\log_{10}(j_*)$ plane. At $z = 0$, galaxies with $b \approx -4$ resemble disk galaxies, and with decreasing b-value the galaxies gradually become more spheroidal, until they clearly resemble elliptical galaxies for $b \leqslant -5$. Therefore, the b-value describes a fundamental connection between three critical parameters in galaxy formation scenarios: the stellar angular momentum j_*, the stellar mass M_*, and the morphology.

This morphological split-up in the M_*–j_* plane is already present at $z = 2$ (Teklu et al. 2016), but shifted towards lower b-values as galaxies generally have a lower stellar specific angular momentum at redshifts higher than $z = 0$. This shift is in good agreement with theoretical predictions of $j_*|_{M_*} \propto \sqrt{z+1}^{-1}$ by Obreschkow et al. (2015). Thus, shifted accordingly, the b-value can be used to classify galaxies up to $z = 2$.

2.1. *Mass–Size Relation*

The left panel of Fig. 1 shows the stellar mass–size plane, color-coded according to the b-value, while the solid and dashed lines mark the observationally found relations for

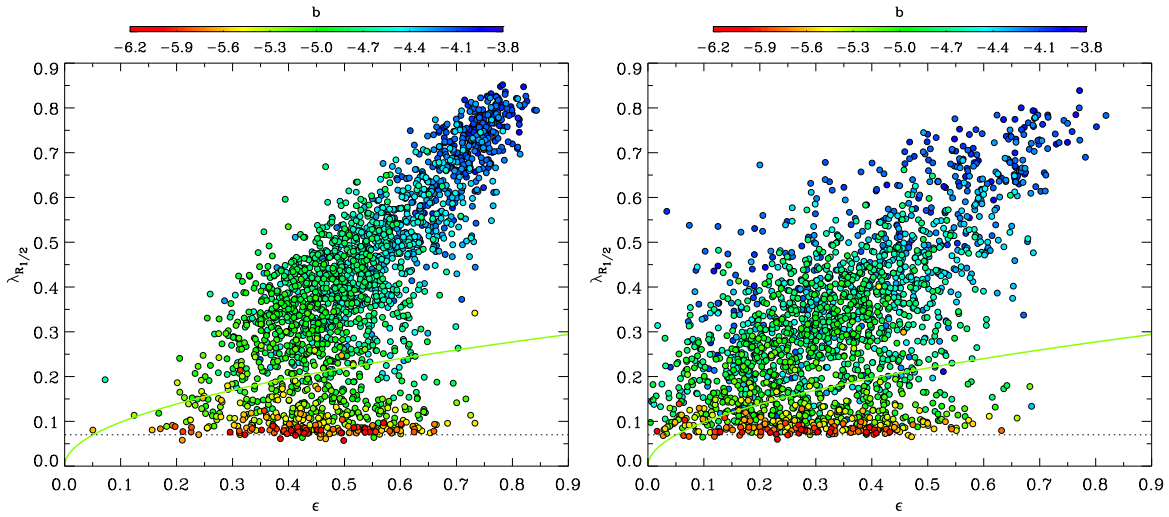

Figure 2. λ_R–ϵ plane for all galaxies from Magneticum Box4, with colors indicating the b-values of the galaxies calculated as in Eq. 2.1, at $z = 0$. The green solid line marks the threshold between slow and fast rotators as defined by Emsellem et al. (2011). *Left panel:* Both λ_R and ϵ are measured for the edge-on projection of each galaxy. *Right panel:* Same as left panel but for random projections.

late-type and early-type galaxies, respectively (Lange et al. 2015). Although Magneticum produces on average slightly larger half-mass radii than found by Lange et al. (2015), we find, for a given stellar mass, a continuous transition from high (disk-like) to low (spheroidal-like) b-values when going from larger to smaller half-mass radii. This confirms that the b-value is an excellent tracer of morphology also in the mass–size plane.

2.2. *Angle between Stellar and Gas Disk Angular Momentum Axes*

The right panel of Fig. 1 shows the distributions of the alignment angles between the angular momentum of the stellar and the gas component, for different b-value bins. While the axes of the galaxies with high b-value (disk-like, blue solid line) are clearly well aligned, the alignment distribution becomes increasingly more random for decreasing b-values, and shows a completely random distribution for spheroidal-like b-values (orange dash-dotted line). This clearly shows that the classification according to the b-value also captures the fact that the stellar and gaseous components of disk galaxies are always aligned, while their orientation can be completely random for spheroidal galaxies (see Teklu et al. 2015 for more details).

2.3. *Kinematical Properties*

Fig. 2 displays the widely used $\lambda_{R_{1/2}}$–ϵ plane (Emsellem et al. 2007), with $\lambda_{R_{1/2}}$ describing the amount of ordered versus random motion and ϵ the ellipticity of a galaxy, for the edge-on projection (left panel) and a random projection (right panel), color-coded according to the b-value. The green solid line marks the fast/slow rotator threshold introduced by Emsellem et al. (2011). In both panels there is a clear trend for the b-value to increase with rising $\lambda_{R_{1/2}}$ and ϵ, although the effect is more pronounced in the edge-on projection. The color gradient evolves continuously along an almost linear relation, indicating a transition from more elliptical-like galaxies towards disk-like morphologies with increasing $\lambda_{R_{1/2}}$ and ϵ, in agreement with observations. Therefore, the b-value also captures the fundamental fast/slow rotator classification (see Schulze et al. 2018 for more details, also with regard to other kinematical properties correlated with the b-value).

3. Conclusions

The Magneticum pathfinder simulations successfully reproduce a large variety of observed galaxy properties, especially the observed distribution of disks and spheroidals in the M_*–j_* plane (e.g., Teklu et al. 2015, 2016). The position of a galaxy in the M_*–j_* plane, characterized by the b-value, is found to be an excellent tracer of morphology. This becomes evident not only in the mass–size plane (see also Dolag et al., in prep.), but also in the distribution of the angles between the angular momentum axes of the gaseous and stellar components of galaxies (see Teklu et al. 2015 for more details). Thus, using the b-value to classify galaxies is an extremely powerful tool for both simulations and observations of galaxies. Furthermore, the b-value is closely correlated to the kinematical λ_R parameter (see Schulze et al. 2018 for more details), clearly demonstrating that those galaxies with the lowest b-values are always slow rotators.

We conclude that the connection between the stellar angular momentum j_* and the stellar mass M_* of a galaxy is a clear indicator for its morphology and thus there exists a clear connection between both quantities and other properties that strongly depend on morphology. Understanding the details of these connections will be a key component in deciphering the formation history of individual galaxies and needs to be studied in more detail in the future.

Acknowledgements

The Magneticum team was supported by the DFG Excellence Cluster "Universe", the Computational Center C^{2}PAP, and the Leibniz-Rechenzentrum (project pr86re).

References

Dolag, K., Borgani, S., Murante, G., & Springel, V. 2009, *MNRAS*, 399, 497
Dolag, K., Vazza, F., Brunetti, G., & Tormen, G. 2005, *MNRAS*, 364, 753
Dolag, K., Jubelgas, M., Springel, V., *et al.* 2004, *ApJL*, 606, L97
Emsellem, E., Cappellari, M., Krajnović, D., *et al.* 2011, *MNRAS*, 414, 888
Emsellem, E., Cappellari, M., Krajnović, D., *et al.* 2007, *MNRAS*, 379, 401
Fall, S. M., & Romanowsky, A. J. 2013, *ApJL*, 769, L26
Hirschmann, M., Dolag, K., Saro, A., *et al.* 2014, *MNRAS*, 442, 2304
Komatsu, E., *et al.* 2011, *ApJS*, 192, 18
Lange, R., Driver, S. P., Robotham, A. S. G., *et al.* 2015, *MNRAS*, 447, 2603
Obreschkow, D., Glazebrook, K., Bassett, R., *et al.* 2015, *ApJ*, 815, 97
Peebles, P. J. E. 1971, *A&A*, 11, 377
Remus, R.-S., Dolag, K., Naab, T., *et al.* 2017, *MNRAS*, 464, 3742
Remus, R.-S., *et al.* 2015, *Galaxies in 3D across the Universe*, 309, 145
Schulze, F., Remus, R.-S., Dolag, K., *et al.* 2018, *MNRAS*, 480, 4636
Springel, V. 2005, *MNRAS*, 364, 1105
Springel, V., Di Matteo, T., & Hernquist, L. 2005, *MNRAS*, 361, 776
Springel, V. & Hernquist, L. 2003, *MNRAS*, 339, 289
Springel, V., White, S. D. M., Tormen, G., & Kauffmann, G. 2001, *MNRAS*, 328, 726
Steinborn, L. K., Dolag, K., Hirschmann, M., *et al.* 2015, *MNRAS*, 448, 1504
Teklu, A. F., Remus, R.-S., Dolag, K., & Burkert, A. 2017, *MNRAS*, 472, 4769
Teklu, A. F., Remus, R.-S., & Dolag, K. 2016, *The Interplay between Local and Global Processes in Galaxies*, 41
Teklu, A. F., Remus, R.-S., Dolag, K., *et al.* 2015, *ApJ*, 812, 29
Tornatore, L., Borgani, S., Dolag, K., & Matteucci, F. 2007, *MNRAS*, 382, 1050